Available online at www.sciencedirect.com
ScienceDirect
Polymer 48 (2007) 3444–3451
polymer
www.elsevier.com/locate/polymer

A temperature-responsive carbon black nanoparticle prepared by surface-induced reversible addition–fragmentation chain transfer polymerization

Qiang Yang [a], Li Wang [a,*], Weidong Xiang [b], Junfeng Zhou [a], Qiao hua Tan [a]

[a] *The State Key Laboratory of Polymer Reaction Engineering, College of Materials Science and Chemical Engineering, Zhejiang University, Hangzhou 310027, People's Republic of China*
[b] *College of Applied Technology, Wenzhou University, Wenzhou 325035, People's Republic of China*

Received 4 November 2006; received in revised form 29 January 2007; accepted 8 February 2007
Available online 7 March 2007

Abstract

A reversible addition–fragmentation chain transfer (RAFT) agent, 2-{[(dodecylsulfanyl)carbonothioyl]sulfanyl}propanoic acid (DSCTSP), was immobilized on the hydroxyl-functionalized carbon black (CB) surface via a direct condensation reaction, producing CB–DSCTSP. Then, RAFT polymerizations were carried out on carbon black surface using the CB–DSCTSP as a chain transfer agent. Poly(*N*-isopropylacrylamide) (PNIPAAm) chains were grown from the carbon black surface by a surface-induced reversible addition–fragmentation chain transfer (SI-RAFT) polymerization. FT-IR, ^{1}H NMR, TGA, TEM, and dynamic light scattering were used to characterize the carbon black grafted with poly(*N*-isopropylacrylamide) (CB-*g*-PNIPAAm). Dispersion experiment showed that CB-*g*-PNIPAAm had a good solubility in water. ^{1}H NMR, AFM and dynamic light scattering measurements showed that CB-*g*-PNIPAAm behaved a reversible temperature-responsive property in water.

Keywords: Carbon black; SI-RAFT polymerization; Temperature-responsive

1. Introduction

Stimuli-responsive hybrid nanoparticles are composed of an inorganic core and a stimuli-responsive polymer shell. Usually, the core part supplies the optical, magnetic, conductive, mechanical properties, and the stimuli-responsive polymer behaves a reversible volume phase transition in response to external stimuli such as changes in temperature, pH and light. Stimuli-responsive hybrid nanoparticles have the potentials for use in photonics, electronics, magnetic devices, sensors, drug delivery, artificial muscles, selective separation membranes, probes, smart coatings, etc. [1–4]. In recent years, temperature-responsive hybrid nanoparticles have attracted much attention, and most studies focused on gold nanoparticles [5–10], silica nanoparticles [11–15], poly(methyl methacrylate) microspheres [16], and polystyrene latex [17]. Carbon-based hybrid materials consisting of stimuli-responsive polymer have been also studied for developing smart materials [18,19]. In fact, carbon black nanoparticle is a relatively conductive material composed of 90–99% elemental carbon, and is most readily available among carbon nanoparticles. And carbon black nanoparticle is a potentially biocompatible and nonimmunogenic material [20]. In general, carbon black nanoparticle has been used in positive temperature coefficient materials, double layer capacitors and gas sensor materials [21–25]. Unfortunately, the applications of carbon black in developing new materials have been studied very little until now. Stone et al. incorporated protein into the poly(vinyl alcohol)/carbon black matrix to translate the change in the protein's conformation as a change in electrical resistance [26]. Akashi et al. found that the poly(*N*-isopropylacrylamide) gel including carbon black nanoparticles was a kind of light-modulation material because PNIPAAm/carbon black gel exhibited a volume phase transition from swollen to shrunken at 34 °C, resulting in a color change below or above 34 °C [27,28].

* Corresponding author. Tel.: +86 571 87953200; fax: +86 571 87951612.
E-mail address: opl_wl@dial.zju.edu.cn (L. Wang).

0032-3861/$ - see front matter © 2007 Published by Elsevier Ltd.
doi:10.1016/j.polymer.2007.02.064

Although carbon black nanoparticle has the concentric graphene layer symmetry with a hydrophobic and low reactive surface, its surface properties can be tailored by grafting polymers, which supplies a great opportunity to develop carbon-based hybrid nanoparticles. Matyjaszewski and co-workers had prepared the water-dispersible carbon black hybrid nanoparticles by surface-initiated atom transfer radical polymerization (SI-ATRP) of 2-(dimethylamino)ethyl methacrylate [29]. Compared with SI-ATRP, surface-induced reversible addition–fragmentation chain transfer (SI-RAFT) polymerization is easy to graft a water-soluble polymer or functional polymer onto a solid surface. To carry out the SI-RAFT polymerization, azoinitiator moieties or RAFT agents need to be immobilized first on a solid surface. Many studies prove that after azoinitiator moieties immobilized on a solid surface, some additional "free" initiators and RAFT agents are necessarily added to a reaction system to carry out the SI-RAFT polymerization [11,12]. Certainly, the RAFT agent may be directly immobilized on a solid surface by Z-group (the activating and radical stabilizing group) or R-group (the leaving and reinitiating group). The SI-RAFT polymerization via a Z-group immobilization approach was reported little [15,30,31]. In spite of side reactions, the R-group immobilization approach is more widely adopted [6,16,9,18,32,33].

PNIPAAm is a typical temperature-responsive polymer that exhibits a reversible and inverse volume phase transition at about 32 °C in water [18]. In this paper, to prepare a kind of temperature-responsive hybrid nanoparticle, PNIPAAm chains were grown from a carbon black nanoparticle surface by the SI-RAFT polymerization.

2. Experimental section

2.1. Materials

Primary carbon black particles (VXC 605), with an average size of 30 nm and a specific surface area of 254 m^2/g, were obtained from Cabot. 1,3-Dicyclohexylcarbodiimide (DCC), dodecanethiol, tetrapropylammonium bromide, 2-bromopropanoic acid, *N*-isopropylacrylamide (NIPAAm) and *N*,*N*-(dimethylamino)pyridine (DMAP) were purchased from Acros. *N*,*N*-Dimethylformamide (DMF) and tetrahydrofuran (THF) were dried with 4 Å molecular sieves before used. Glycol was freshly distilled before use to remove little water, and thionyl chloride ($SOCl_2$) and nitric acid (HNO_3) were used as received.

2.2. Characterization

^{1}H NMR spectra were recorded with a 400 MHz AVANCE NMR spectrometer (Model DMX400). Fourier-transform infrared (FT-IR) spectra were recorded on a Jasco IR-700 infrared spectrophotometer. Thermogravimetric analysis (TGA) was performed on a Perkin–Elmer TGA-7 (heating rate of 20 °C/min, from 25 °C to 800 °C, in a flow of nitrogen). The hydrodynamic diameters of particles were measured by dynamic light scattering (Zetasizer 3000, Malvern Instruments, wavelength 633 nm, count rate 240.9, Cell Type Capillary cell, power 70 mW, detector angle 90°). Transmission electron microscopic (TEM) images were obtained from a JEOL model 1200EX instrument operated at an accelerating voltage of 160 keV. Scanning electron microscopic (SEM) image was obtained from a JEOL 6700F field-emission microscope operated at an acceleration voltage of 10 keV. Atom force microscopic (AFM) measurements were carried out with the aid of a Nanoscope III equipped with phase extender module and vertical engage J scanner. The images were acquired in the tapping mode under ambient conditions with standard silicon cantilevers with a nominal spring constant of 50 N/m and a resonance frequency around 300 kHz.

2.3. Experimental procedures

2.3.1. Synthesis of 2-{[(dodecylsulfanyl)carbonothioyl]-sulfanyl}propanoic acid (DSCTSP) [34]

In an ice bath, 0.50 g (12.5 mmol) NaOH was dissolved in a mixture of 3.0 mL (12.5 mmol) dodecanethiol, 40 mL (0.54 mol) acetone, 5 mL (0.28 mol) water, and 0.27 g (0.10 mmol) tetrapropylammonium bromide. Then 0.75 mL (12.5 mmol) carbon disulfide was dripped into the resulting mixture, and 1.13 mL (12.5 mmol) 2-bromopropanoic acid was also added after 30 min. The mixture was stirred at room temperature for overnight. Then, the solution was evaporated and slowly acidified with 50 mL 2 M hydrochloric acid. The precipitate was collected and recrystallized from ether–light petroleum gaining yellow solid. ^{1}H NMR (400 MHz, $CDC1_3$): δ 4.86 (1H, $-SCHCH_3-$), 3.36 (2H,$-CH_2S-$), 1.70 (2H, $-CH_2CH_2S-$), 1.64 (3H, $-SCHCH_3-$), 1.40 (2H, $-CH_2CH_2CHS-$), 1.2–1.34 (16H, $CH_3(CH_2)_8-$), 0.88 (3H, CH_3CH_2-).

2.3.2. Introducing hydroxyl group onto carbon black surface (CB–OH) [35]

A suspension of carbon black (2.0 g, 0.1753 mol C) and 65% nitric acid (20 mL, 0.293 mol) was sonicated for 30 min and was stirred for 24 h at 100 °C. After cooling to room temperature, the product was separated by vacuum filtration and washed with deionized water until the pH reached 7. The resultant product was dried in vacuum at 50 °C, giving 1.2 g CB–COOH (1.68 mmol/g, –COOH).

CB–COOH (2.016 mmol, –COOH) of 1.2 g was dispersed in 50 mL $SOCl_2$ (0.685 mol) and the mixture was stirred at 65 °C for 24 h. After the residual $SOC1_2$ was removed by vacuum, 20 mL glycol (0.36 mol) was added and stirred at 120 °C for 24 h. The resultant solid was separated by vacuum filtration and completely washed with deionized water and THF. The resultant product was dried in vacuum at 50 °C, obtaining 0.6208 g CB–OH (1.41 mmol/g, –OH).

2.3.3. Immobilizing the RAFT agent on carbon black surface (CB–DSCTSP) [9]

CB–OH (0.79 mmol, –OH) of 0.5606 g, 0.2189 g DSCTSP (0.63 mmol), 74.5 mg DMAP (0.61 mmol) and 0.1306 g DCC (0.63 mmol) were added into a 25 mL

three-necked flask, and the mixture was sonicated in 10 mL DMF for 30 min. The mixture was reacted for 1 h at 0 °C, and further reacted for 48 h at room temperature. The product was separated centrifugally (each time for 30 min with the rotation speed 3000 r/min), and was completely washed with ethanol, deionized water and THF to remove any possible absorbed DSCTSP. The resultant product was dried in vacuum at 50 °C, obtaining CB–DSCTSP (0.33 mmol/g, the RAFT agent).

2.3.4. Synthesis of CB-g-PNIPAAm

Typically, 50 mg CB–DSCTSP (16.5 μmol, the RAFT agent), 0.4 mg AIBN (2.4 μmol) and 0.5051 g NIPAAm (4.46 mmol) and 3 mL 1,4-dioxane were placed in a 25 mL two-necked flask, degassed with three freeze–thaw cycles. The flask was immersed in an oil bath at 80 °C for 24 h. At the end of reaction, the resultant product was separated centrifugally (each time for 30 min with rotation speed 3000 r/min), and was washed with deionized water and THF. Such procedures were repeated until there was no white sediment detected in the supernatant solution by the addition of ether. The resultant product was dried in vacuum at 50 °C.

3. Results and discussion

3.1. Immobilizing the RAFT agent on carbon black surface

A reversible addition and fragmentation chain transfer (RAFT) agent, 2-{[(dodecylsulfanyl)carbonothioyl]sulfanyl}-propanoic acid was immobilized on the hydroxyl-activated carbon black nanoparticle surface through a direct condensation reaction with its surface hydroxyl group. First, pristine carbon black was oxidized with HNO_3 to produce carboxylic groups. Then, the carboxylic group on the carbon black surface was reacted with thionyl chloride and subsequently was reacted with glycol to introduce hydroxyl group. The hydroxyl group on the carbon black surface was reacted with 2-{[(dodecylsulfanyl)carbonothioyl]sulfanyl}propanoic acid via a condensation reaction. Scheme 1 illustrates the process of immobilizing the RAFT agent on carbon black surface.

The whole process of immobilizing the RAFT agent on carbon black surface can be verified by TGA, EDS and FT-IR. Fig. 1 shows the TGA curves of carbon black, CB–COOH, CB–OH and CB–DSCTSP. Pristine carbon black remained basically stable up to 685 °C and had about 6.19% between 25 °C and 800 °C. CB–COOH had about 7.58% weight loss

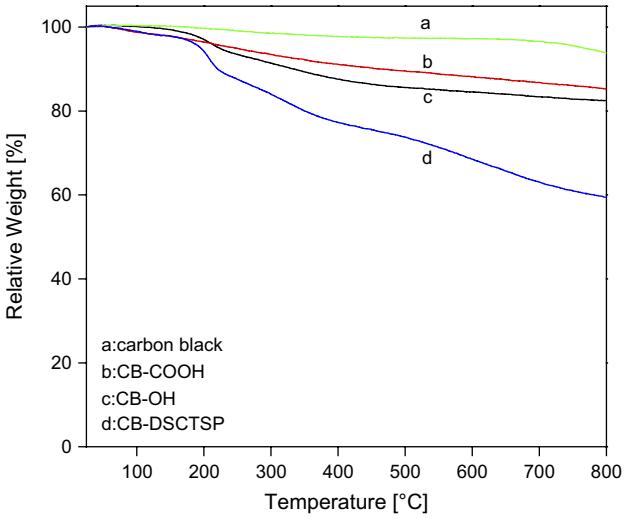

Fig. 1. TGA curves of carbon black, CB–COOH, CB–OH and CB–DSCTSP.

below 300 °C and the carboxyl group's density was approximately 1.68 mmol/g, calculated by TGA. CB–OH had about 13.80% weight loss below 460 °C [35] and the hydroxyl group's density was about 1.41 mmol/g. CB–DSCTSP had about 24.80% weight loss below 460 °C and the RAFT agent group's density was 0.33 mmol/g.

Energy dispersive spectroscopy (EDS) was used to further characterize the CB–DSCTSP. Fig. 2 shows the EDS of CB–DSCTSP. A weak sulfur peak can be detected in CB–DSCTSP, which is assigned to the sulfur bond of the 2-{[(dodecylsulfanyl)carbonothioyl]sulfanyl}propanoic acid.

Fig. 3 shows the FT-IR spectra of carbon black, CB–COOH, CB–OH and CB–DSCTSP. For the CB–COOH sample, the peak at 1793 cm^{-1} assigned to the stretching vibration of carbonyl group (C=O) was much stronger than that of carbon black. For the CB–OH sample, the peak at 3426 cm^{-1} assigned to the stretching vibration of hydroxyl group (–OH) was more obvious. The two characteristic peaks of the RAFT agent were, respectively, at 1718 cm^{-1} assigned to the vibration of C=O and at 1088 cm^{-1} attributed to the vibration of C=S [18].

3.2. Synthesis of CB-g-PNIPAAm

Recently, Pan and co-workers reported that PNIPAAm was grafted onto multiwalled carbon nanotubes by surface RAFT polymerization with dithiobenzoate as the RAFT agent [18]. Here, growing PNIPAAm chains from carbon black surface

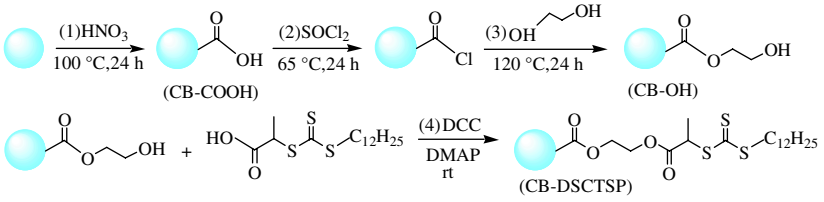

Scheme 1. Synthetic route of immobilizing the RAFT agent on carbon black surface.

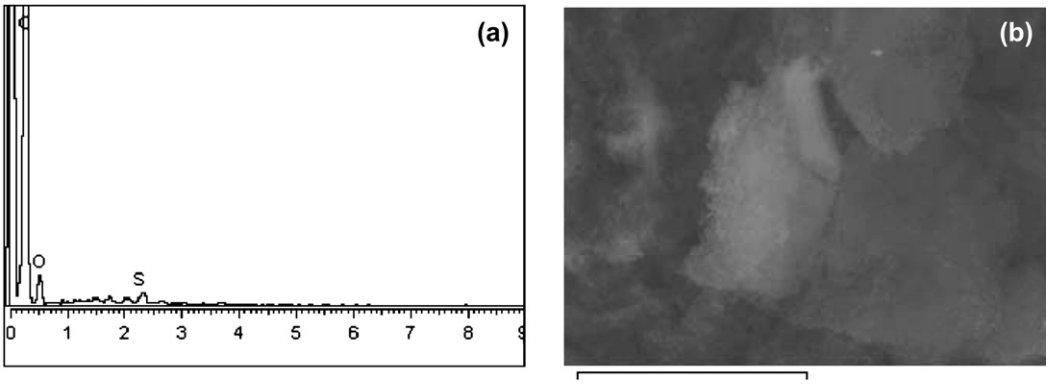

Fig. 2. Energy dispersive spectroscopy spectrum (a) and SEM (b) of CB–DSCTSP. The scale is 30 μm.

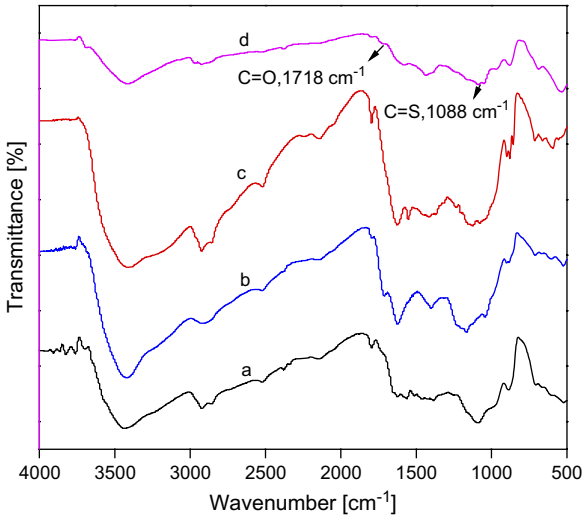

Fig. 3. FT-IR spectra of carbon black, CB–COOH, CB–OH and CB–DSCTSP. (a) Carbon black, (b) CB–OH, (c) CB–COOH, (d) CB–DSCTSP.

by SI-RAFT polymerization are illustrated in Scheme 2. All polymerizations were conducted at 80 °C in 1,4-dioxane. Here, the amount of the RAFT agent was 16.5 μmol, and the initiator (AIBN) was 2.4 μmol. In a typical polymerization, 50 mg CB–DSCTSP, 3 mL 1,4-dioxane, 0.4 mg AIBN and 0.5 g NIPAAm were added into a 25 mL two-necked flask. The flask was evacuated and back-filled with argon three times. After polymerization at 80 °C for 24 h, the reaction solution became thick, which suggested that the SI-ATRP had taken place. The polymerization was quenched by exposure to air. Then, the reaction solution was diluted with water, and was centrifuged at 3000 rpm for 30 min to remove unreacted monomer and un-grafted polymer. The sediment was redispersed into water under ultrasonic, such centrifugation–redispersion cycles were repeated until there was no white

Table 1
Reaction conditions and results

Sample	R_1	R_2	Temp (°C)	Time (h)	F_{wt} (%)
CB-*g*-PNIPAAm-1	10:1	1858:6.9:1	80	8	53.0
CB-*g*-PNIPAAm-2	10:1	1858:6.9:1	80	12	61.6
CB-*g*-PNIPAAm-3	10:1	1858:6.9:1	80	24	79.9
CB-*g*-PNIPAAm-4	10:1	1858:6.9:1	80	36	84.1

Reaction conditions: 50 mg CB–DSCTSP, 0.5 g NIPAAm, 0.4 mg AIBN, 3 mL 1,4-dioxane, 80 °C. R_1 = monomer:CB–DSCTSP (wt:wt). R_2 = monomer:the RAFT agent:AIBN (mol:mol:mol). F_{wt} (%) = the polymer content, calculated from TGA under N_2.

sediment detected in the supernatant solution after the addition of ether. Detailed experimental conditions and results are listed in Table 1.

The relative content of grafted PNIPAAm onto carbon black surface, compared with pristine carbon black, was determined from thermogravimetric analysis (TGA). Fig. 4 shows one major decomposition region at 320–450 °C corresponding to PNIPAAm. The content of PNIPAAm grafted onto carbon black surface varied from 53.0% to 84.1% with the increase of reaction time. It was noted that there was a sharp increase in the amount of PNIPAAm when grafted from 12 h to 24 h. Maybe, the heterogenous surface polymerization reaction was responsible for the sharp increase of PNIPAAm grafted. Thus, changing the reaction time could control the content of PNIPAAm grafted onto carbon black surface.

Fig. 5 shows the FT-IR spectra of CB-*g*-PNIPAAm. The two peaks at 3311 cm^{-1} and 1536 cm^{-1} were assigned to the vibration of the N–H bond, and an obvious peak at 1642 cm^{-1} was attributed to the vibration of carboxyl group. The characteristic double peaks at 1448 cm^{-1} and 1370 cm^{-1} indicated the presence of the isopropyl group [18].

Morphology of CB-*g*-PNIPAAm was studied by transmission electron microscopy (TEM). The sample was prepared

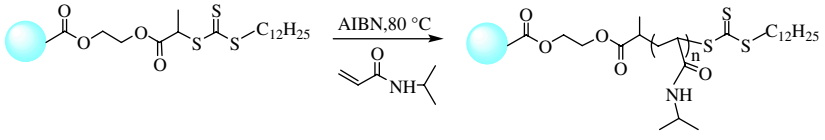

Scheme 2. Synthesis of CB-*g*-PNIPAAm by SI-RAFT.

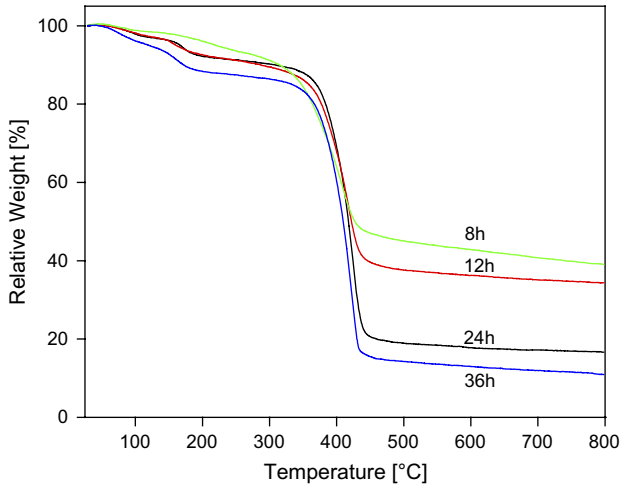

Fig. 4. TGA curves of CB-*g*-PNIPAAm.

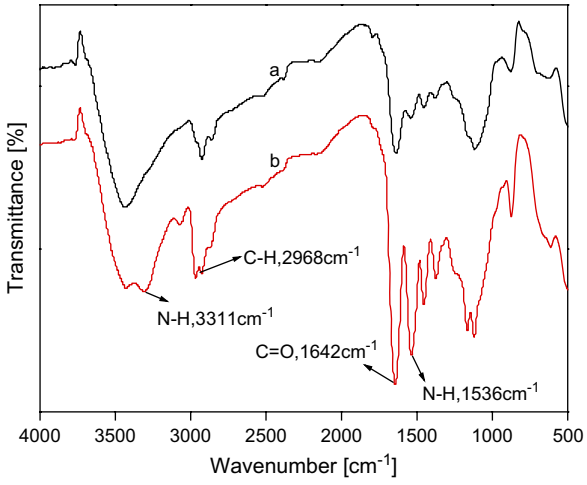

Fig. 5. FT-IR spectra of CB-*g*-PNIPAAm. (a) CB-*g*-PNIPAAm-1, (b) CB-*g*-PNIPAAm-3.

at room temperature. Fig. 6 shows the TEM images of CB-*g*-PNIPAAm in water. As well known, carbon black is strongly hydrophobic in water. After grafting PNIPAAm, carbon black can be well dispersed in water. CB-*g*-PNIPAAm mostly formed nanometer-sized agglomerates in water. The average

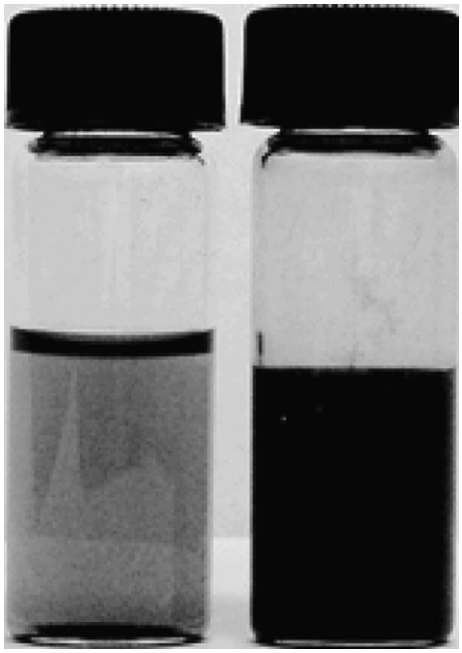

Fig. 7. Solubility photo of carbon black (left) and CB-*g*-PNIPAAm (right) in water.

diameter of CB-*g*-PNIPAAm was about 400 nm, which was consistent with the result by dynamic light scattering.

Under the lower critical solution temperature (LCST) at about 32 °C, PNIPAAm is soluble in water because it can form the intermolecular hydrogen bonding with water molecule [19]. CB-*g*-PNIPAAm formed the core–shell structure, in which the PNIPAAm shell could supply steric stabilization in water. As a result, CB-*g*-PNIPAAm has a good solubility and stability in water at room temperature. And after placed for three months, there was no obvious sedimentation observed, as shown in Fig. 7.

3.3. Temperature-responsive property of CB-g-PNIPAAm

It is well known that PNIPAAm with LCST at about 32 °C behaves temperature-responsive property in water. Below the LCST, PNIPAAm will form the intermolecular hydrogen

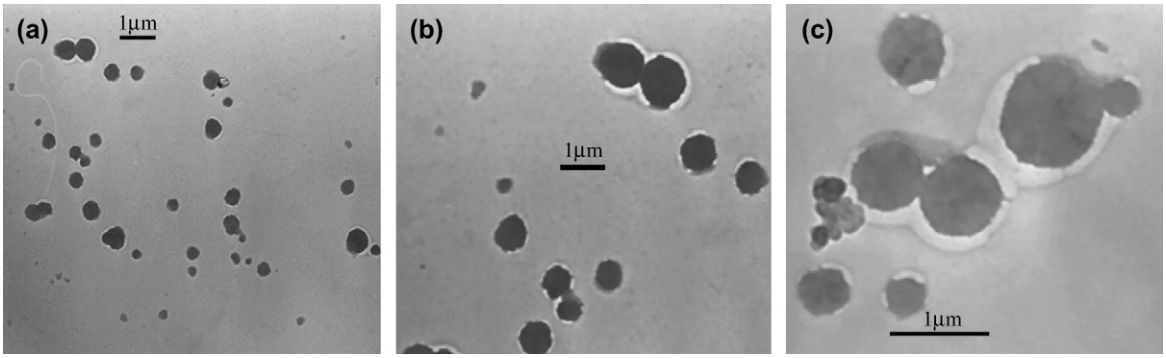

Fig. 6. TEM images at different magnifications of CB-*g*-PNIPAAm in water. Sample was dried at room temperature.

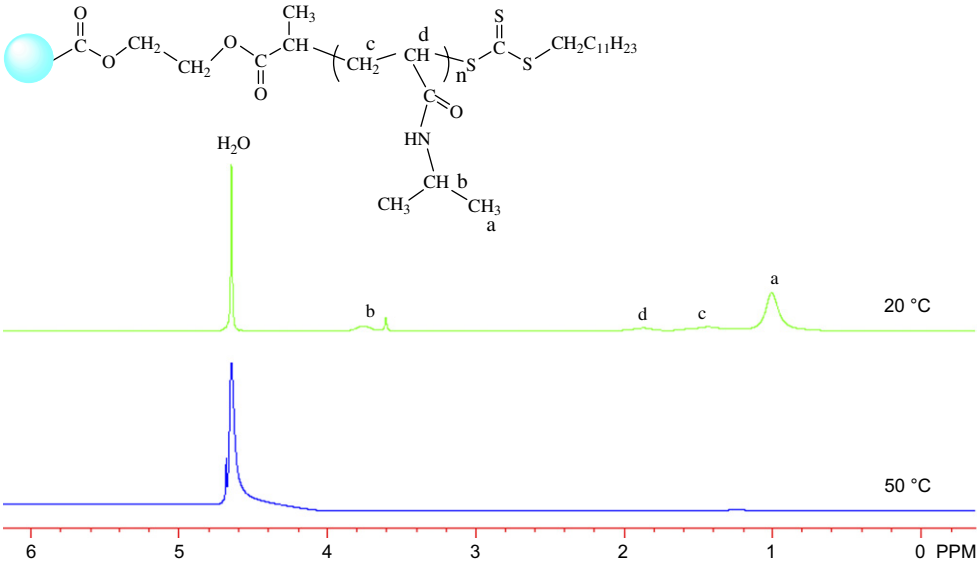

Fig. 8. ^{1}H NMR spectra of CB-*g*-PNIPAAm in D_2O at different temperatures.

bonding with water molecules and can be soluble in water owing to the loosely coiled-structure chains. Above the LCST, PNIPAAm will behave hydrophobic because of the intermolecular hydrogen bonding between C═O and N—H groups within the molecular chains, as a result, PNIPAAm will precipitate gradually from water [6,18,19]. Similar to temperature-responsive property of PNIPAAm in solution, many studies proved that hybrid nanoparticles with PNIPAAm shells behaved temperature-responsive property in water [5–17]. Li et al. synthesized thermosensitive gold nanoparticles exhibiting a sharp, reversible, clear-opaque transition in solution between 25 °C and 30 °C [6]. Deng and Sun reported that PNIPAAm-encapsulated polystyrene latex underwent a dramatic volume decrease at LCST of PNIPAAm [17].

In our experiment, a sample with higher concentration of CB-*g*-PNIPAAm formed stable dispersion in water at 20 °C, while deposited quickly from water at 50 °C. The result approximately showed that CB-*g*-PNIPAAm had temperature-responsive in water between 20 °C and 50 °C. To study in detail temperature-responsive property of PNIPAAm, temperature-variable ^{1}H NMR was used to verify the temperature-responsive property of PNIPAAm. At each temperature, the dispersion containing CB-*g*-PNIPAAm was equilibrated for 30 min. Fig. 8 shows the ^{1}H NMR spectrum of CB-*g*-PNIPAAm in D_2O at different temperatures. The corresponding hydrogen signals of PNIPAAm units could be obviously observed at 20 °C. When the temperature rose to 50 °C, the corresponding hydrogen signals disappeared because CB-*g*-PNIPAAm underwent the extended hydrophilic to globular hydrophobic transition.

The temperature-responsive property of CB-*g*-PNIPAAm in water was further investigated by variable-temperature dynamic light scattering (DLS). While DLS measurements are not very accurate as they are performed at 90°, variable-temperature DLS is one of the powerful tools to characterize the temperature-responsive property of PNIPAAm. Fig. 9 shows the size changes of CB-*g*-PNIPAAm with the increase of temperature. At one temperature, the dispersion was equilibrated for 30 min. It was obvious that a sudden change took place at about 32 °C, which was consistent with the LCST of pure PNIPAAm. With the further increase of temperature, CB-*g*-PNIPAAm nanoparticle became smaller. PNIPAAm chains on carbon black surface underwent an extended hydrophilic to globular hydrophobic transition resulting in collapse of chains, which was responsible for the decrease in size. Fig. 10 illustrates the collapse of PNIPAAm molecular chains on carbon black surface induced by the transition from hydrophilic to hydrophobic. The maximum diameter change was about 100 nm between 10 °C and 50 °C. Deng et al. found that the maximum diameter change was about 72 nm for PNIPAAm-encapsulated polystyrene latex from 28 °C to 50 °C. Higher PNIPAAm grafting density could be responsible for the relative great change in size. In fact, change in size of CB-*g*-PNIPAAm was smaller than that of pure PNIPAAm because the former interchain interactions in water were not strong [19]. The change in size distribution of CB-*g*-PNIPAAm also showed the transition. During the DLS experiments, no any sediment could be observed at temperature above LCST, possibly due to the low concentration [7]. Under low concentration condition, it was maybe little chance for carbon black nanoparticles to collide with each other and produce great aggregates.

Fig. 11 shows the hydrodynamic number-averaged diameter changes of CB-*g*-PNIPAAm with temperature fluctuation. More important is that the size changes of CB-*g*-PNIPAAm are almost repeatable, and precipitates cannot be observed in the heating and cooling cycle. The reversible change in size endowed CB-*g*-PNIPAAm nanoparticle is a kind of temperature-switching properties. Similar repeatable phenomena could be observed in thermosensitive gold nanoparticles and temperature-responsive carbon nanotube hybrids [6,18]. Ding et al. found that PNIPAAm blocks in water also retained their

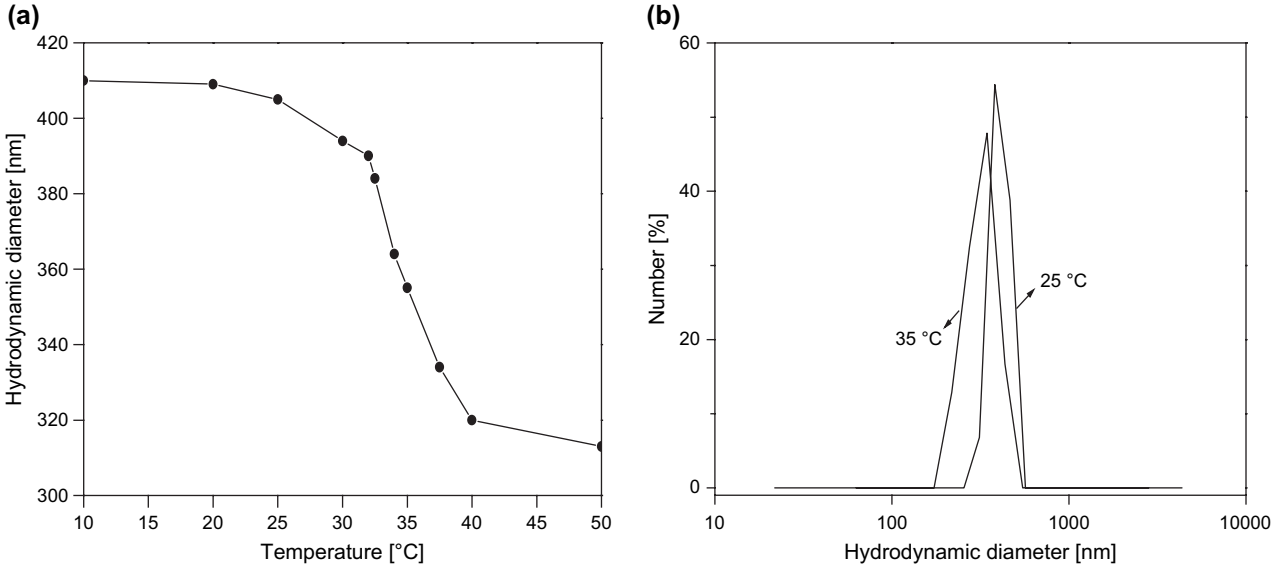

Fig. 9. Temperature dependence of the hydrodynamic number-averaged diameter (a) and size distribution (b) of CB-*g*-PNIPAAm in water.

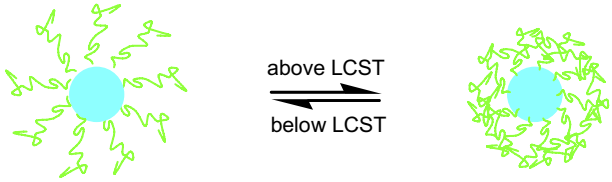

Fig. 10. Schematic illustration of temperature-responsive property of CB-*g*-PNIPAAm in water.

swelling/shrinking and hydrophilic/hydrophobic properties intact when underwent repeated temperature changes [36].

The temperature-responsive property of CB-*g*-PNIPAAm was further verified by atom force microscope (AFM). Fig. 12 shows the AFM images of CB-*g*-PNIPAAm at 25 °C and 50 °C. The CB-*g*-PNIPAAm sample prepared at 25 °C mostly existed with nano-sized agglomerates, while the sample prepared at 50 °C showed large agglomerates with micrometer scale. The AFM result also verified the extended hydrophilic to globular hydrophobic transition. Below the LCST, PNIPAAm chains on carbon black particle surface

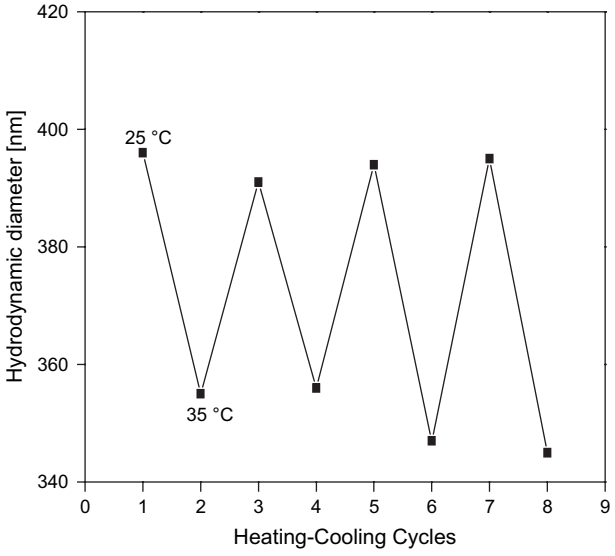

Fig. 11. Hydrodynamic number-averaged diameter changes of CB-*g*-PNIPAAm with temperature fluctuation.

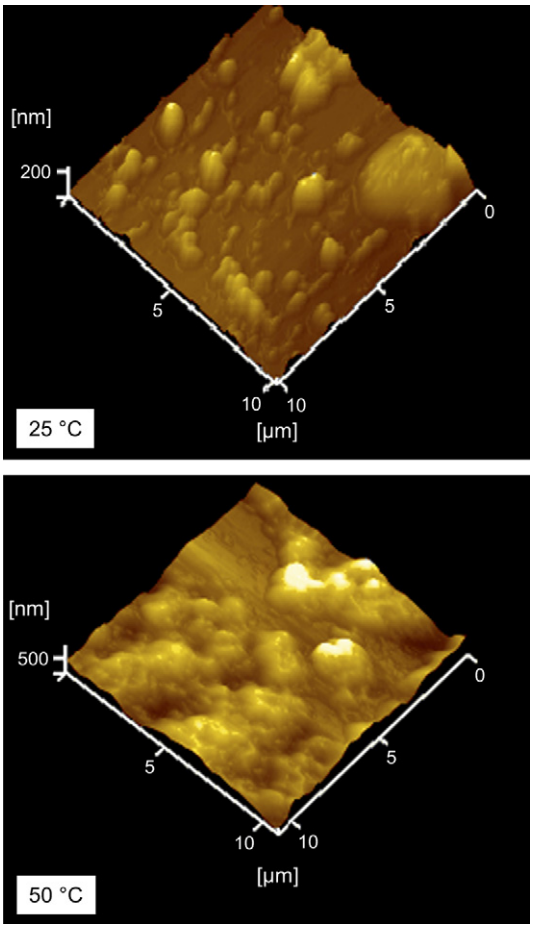

Fig. 12. AFM images of CB-*g*-PNIPAAm at 25 °C (top) and at 50 °C (bottom).

mostly formed the hydrogen bonding with water molecule. Above the LCST, the hydrogen bonding between PNIPAAm and water was destroyed and formed the new intermolecular hydrogen bonding among these PNIPAAm chains. Gao and co-workers studied the temperature-responsive properties of PNIPAAm-coated carbon nanotubes with AFM [19].

4. Conclusions

PNIPAAm chains were grown from carbon black nanoparticle surface by surface-induced reversible addition–fragmentation chain transfer polymerization. CB-*g*-PNIPAAm formed the core–shell structure with PNIPAAm shells and behaved reversible temperature-responsive property in water. Such a kind of temperature-responsive hybrid nanoparticle maybe have the potential applications in smart sensor, temperature-switching materials, etc.

References

[1] Templeton AC, Wuelfing WP, Murray RW. Acc Chem Res 2000;33:27–36.
[2] Annaka M, Tanaka T. Nature 1992;355:430–2.
[3] Tanaka T, Nishio I, Sun ST, Nishio SU. Science 1982;218:467–9.
[4] Suzuki A, Tanaka T. Nature 1990;346:345–7.
[5] Shan J, Nuopponen M, Jiang H, Viitala T, Kauppinent E, Kontturi K, et al. Macromolecules 2005;38:2918–26.
[6] Zhu MQ, Wang LQ, Exarhos GJ, Li ADQ. J Am Chem Soc 2004;126:2656–7.
[7] Suzuki D, Kawaguchi H. Langmuir 2005;21:8175–9.
[8] Kaholek M, Lee WK, Ahn SJ, Ma HW, Caster KC, Mattina BL, et al. Chem Mater 2004;16:3688–96.
[9] Raula J, Shan J, Nuopponen M, Niskanen A, Jiang H, Tenhu H, et al. Langmuir 2003;19:3499–504.
[10] Sumerlin BS, Lowe AB, Stroud PA, Zhang P, Urban MW, McCormick CL. Langmuir 2003;19:5559–62.
[11] Zhai GQ, Yu WH, Kang ET, Neoh KG. Ind Eng Chem Res 2004;43:1673–80.
[12] Yu WH, Kang ET, Neoh KG. Ind Eng Chem Res 2004;43:5194–202.
[13] Li DJ, Jones GL, Dunlap JR, Hua FJ, Zhao B. Langmuir 2006;22:3344–51.
[14] Peng Q, Lai DMY, Kang ET, Neoh KG. Macromolecules 2006;39:5577–82.
[15] Baum M, Brittain WJ. Macromolecules 2002;35:610–5.
[16] Li CZ, Han JW, Ryu CY, Benicewicz BC. Macromolecules 2006;39:3175–83.
[17] Sun QH, Deng YL. Langmuir 2005;21:5812–6.
[18] Hong CY, You YZ, Pan CY. Chem Mater 2005;17:2247–54.
[19] Kong H, Li WW, Gao C, Yan DY, Jin YZ, Walton RM, et al. Macromolecules 2004;37:6683–6.
[20] Yan AH, Lau BW, Weissman BS, Külaots I, Yang NYC, Kane AB, et al. Adv Mater 2006;18:2373–8.
[21] Li JR, Xu JR, Zhang MQ, Rong MZ. Carbon 2003;41:2353–60.
[22] Chen SG, Hu JW, Zhang MQ, Li MW, Rong MZ. Carbon 2004;42:645–51.
[23] Xie HF, Yang QD, Sun XX, Yang JJ, Huang YP. Sens Actuators B Chem 2006;113:887–91.
[24] Chen JH, Tsubokawa N, Maekawa Y, Yoshida M. Carbon 2002;40:1597–617.
[25] Richner R, Müller S, Wokaun A. Carbon 2002;40:307–14.
[26] Brott LL, Rozenzhak SM, Naik RR, Davidson SR, Perrin RE, Stone MO. Adv Mater 2004;16:592–6.
[27] Akashi R, Tsutsui H, Komura A. Adv Mater 2002;14:1808–11.
[28] Tsutsui H, Moriyama M, Nakayama D, Ishii R, Akashi R. Macromolecules 2006;39:2291–7.
[29] Liu TQ, Jia SJ, Kowalewski T, Matyjaszewski K. Macromolecules 2006;39:548–56.
[30] Perrier S, Takolpuckdee P, Mars CA. Macromolecules 2005;38:6770–4.
[31] Hernández-Guerrero M, Barner-Kowollik C, Davis TP, Stenzel MH. Eur Polym J 2005;41:2264–77.
[32] Stenzel MH, Zhang L, Huck WTS. Macromol Rapid Commun 2006;27:1121–6.
[33] Hong CY, You YZ, Pan CY. J Polym Sci Part A Polym Chem 2005;44:2419–27.
[34] Ferguson CJ, Hughes RJ, Nguyen D, Pham BTT, Gilbert BG, Hawkett BS, et al. Macromolecules 2005;38:2191–204.
[35] Kong H, Gao C, Yan DY. J Am Chem Soc 2004;126:412–3.
[36] Chen XG, Ding XB, Zheng ZH, Peng YX. New J Chem 2006;30:577–82.